

Influence of the atomic scale inhomogeneity of the pair interaction on the local pair formation and density of states in high- T_c superconductors.

A. M. Bobkov and I. V. Bobkova*

Institute of Solid State Physics, Chernogolovka, Moscow reg., 142432 Russia

(Dated: February 9, 2022)

The influence of the atomic-scale inhomogeneities of the pairing interaction on the superconducting order parameter distribution and the LDOS is studied in the framework of mean-field BCS theory for two-dimensional lattice model. It is found that the ratio of the local low-temperature gap in differential conductance to the local temperature of vanishing the gap $2\Delta_g/T_p$ can take large enough values compared to the homogeneous case. This ratio practically does not depend on the location in the sample and is independent on the concentration of local pair interaction perturbations in wide range of concentrations. The obtained results could bear a relation to the recent measurements by Gomes *et. al*¹.

PACS numbers: 74.20.Fg, 74.25.Jb, 74.72.-h

Nanoscale inhomogeneities have been widely observed in the high-temperature superconductor $\text{Bi}_2\text{Sr}_2\text{CaCu}_2\text{O}_{8+x}$ (BSCCO) and have generated intense interest^{2,3,4,5,6,7}. In particular, the spectral gap in the local density of states (LDOS) has been investigated by scanning tunneling microscopy (STM). It was found that the gap varies by a factor of 2 over distances of 20 – 30 Å. These observations have been made primarily in the superconducting state. Several scenarios have been proposed to understanding this electronic inhomogeneity. First of all, it was speculated that poorly screened electrostatic potentials of the dopant atoms vary a doping concentration locally, giving rise to the gap modulations^{8,9,10}. Alternatively, these inhomogeneities are associated with a competing order parameter^{11,12,13,14,15,16}. Further, the positive correlations between the inhomogeneities and positions of the dopant atoms have been observed by STM on the optimally doped BSCCO⁶. After that it was proposed by Nunner *et al.*¹⁷ that the dopant atoms modulate the pairing interaction locally on the atomic scale. The LDOS calculated in the framework of this model is in good agreement with the key characteristics of the experimental data. In addition, finite-temperature order parameter evolution was investigated and the specific heat was calculated within the same model¹⁸.

On the other hand, it is well known that in the high- T_c superconductors a partial gap in the LDOS exists for a range of temperatures above T_c ¹⁹. There is no consensus up to now if this gap is due to pairing without phase coherence, a competing order or proximity to the Mott state^{20,21,22,23}. The inhomogeneities described above complicate the situation. Only very recently the spatially resolved STM measurements of gap formation in BSCCO samples were performed¹. For a range of doping from 0.16 to 0.22 they have found that gaps nucleate in nanoscale regions above T_c and proliferate as the temperature is lowered, evolving to the spatial distribution of gap values in the superconducting state. It was observed experimentally that overdoped and optimally doped samples have identical gap-temperature scaling ra-

tios, which together with the fact that in the overdoped samples pseudogap effects are believed to be weak or absent, allowed Gomes *et. al* to interpret the gaps above T_c as those associated with pairing. The most striking experimental observation is that, despite the inhomogeneity, every pairing gap develops locally at the temperature T_p following the relation $2\Delta/T_p = 7.9 \pm 0.5$ in wide range of doping from overdoped to optimally doped samples. So large and independent on the size of local gap values ratio $2\Delta/T_p$ seems to be different from the expectations based on the BCS theory and its strong-coupling extension, where it is in the range 3.5 – 5 and becomes dependent on Δ .

In the present paper we show that if the pairing interaction is modulated locally on the atomic scale, as it was proposed by Nunner *et. al*¹⁷, the ratio $2\Delta/T_p$ strongly increases in the framework of conventional BCS theory. This is in sharp contrast to the influence of the potential disorder, which, as was demonstrated²⁴, can only diminish this quantity. It is found that the ratio $2\Delta/T_p$ is practically independent on the number of off-diagonal (pairing interaction) scatterers, which is proportional to the doping in the model by Nunner *et. al*¹⁷, in a wide range of concentrations. We obtained the ratio $2\Delta/T_p$ to be position-independent in case if the off-diagonal scatterers are distributed rather uniformly and equal to 5.9. For comparison, the ratio $2\Delta/T_p = 4.7$ for the homogeneous sample corresponding to the lattice parameters we use (it is slightly higher than the ratio $2\Delta/T_c = 4.3$, because T_p is smaller than the mean-field critical temperature T_c as it is discussed below). These results are reminiscent of the measurements by Gomes *et. al*¹ except for the fact that the ratio $2\Delta/T_p$ we calculated is about thirty percent smaller than experimentally measured one. On the other hand, the ratio $2\Delta_g/T_p$ is found to be very sensitive to characteristic size and height of the individual pairing interaction scatterer and especially to the choice of the lattice parameters and can be further increased manipulating by these quantities. It is worth noting that our analysis is phenomenological and the conclusions are independent on the underlying pairing mechanism and

the particular course of the local pair interaction modulations.

Model and method.—We consider the following mean-field Hamiltonian on a square lattice

$$\hat{H} = - \sum_{\langle ij \rangle, \sigma} t_{ij} c_{i\sigma}^\dagger c_{j\sigma} - \sum_{i, \sigma} \mu c_{i\sigma}^\dagger c_{j\sigma} + \sum_{\langle ij \rangle} (\Delta_{ij} c_{i\uparrow}^\dagger c_{j\downarrow}^\dagger + h.c.), \quad (1)$$

where $c_{i\sigma}$ ($c_{i\sigma}^\dagger$) stands for an electron annihilation (creation) operator at site i with spin σ . $\sum_{\langle ij \rangle}$ indicates summation over neighboring sites, t_{ij} is the hopping integral between sites i and j . We set t_{ij} to be $t = 1$ for the nearest-neighbor hopping, $t' = -0.3$ for the next nearest-neighbor hopping and $t'' = 0.1$ for the next-next one. μ is adjusted to be -1 to model the Fermi surface of BSCCO near optimal doping. Below all the energies are measured in units of t . The nearest-neighbor d -wave order parameter (OP) should be determined self-consistently: $\Delta_{ij} = -g_{ij} \langle c_{i\downarrow} c_{j\uparrow} - c_{j\downarrow} c_{i\uparrow} \rangle$. Following Ref. 17 we model the inhomogeneous pairing interaction by $g_{ij} = g_b + \delta g (f_i + f_j)/2$, where g_b corresponds to an average background interaction and $f_i = \sum_s \exp(-r_{is}/\lambda)/r_{is}$, where r_{is} is the distance between the site i and the source of the pairing interaction perturbation. The mean-field BCS treatment is generally believed to be appropriate for overdoped (and, to some extent, optimally doped) samples. So, we do not consider underdoped regime, where the proximity to the Mott state should be taken into account.

In order to analyze the inhomogeneous pairing correlations in the framework of the mean-field hamiltonian (1) we exploit the fully self-consistent T-matrix technique for Gor'kov Green's functions. The full Green's function takes the form

$$\check{G}_{ij} = \check{G}_{ij}^0 + \sum_{k,m} \check{G}_{ik}^0 \check{T}_{km} \check{G}_{mj}^0. \quad (2)$$

Here $\check{T}_{km} = -\sum_n (\check{M}^{-1})_{kn} \check{V}_{nm}$, $\check{M}_{km} = \delta_{km} + \sum_n \check{G}_{kn}^0 \check{V}_{nm}$. In this paper we only focus on the off-diagonal self-energy inhomogeneity and therefore $\check{V}_{km} = \delta \Delta_{km} i \hat{\sigma}_2 i \hat{\tau}_2$. All Green's functions and T-matrices are 4×4 matrices in the direct product of spin and particle-hole spaces, what indicated by the symbol $\check{\cdot}$. $\hat{\tau}_i$ and $\hat{\sigma}_i$ are Pauli matrices in particle-hole and spin spaces respectively. The summation is taken over all the sites, where the OP $\Delta_{km} = \Delta_{km}^0 + \delta \Delta_{km}$ differs from the background value Δ_{km}^0 . Δ_{km}^0 is assumed to be of d -wave type, that is $\Delta_{i\pm\hat{a}}^0 = -\Delta_{i\pm\hat{b}}^0 = \Delta^0$. \hat{a} and \hat{b} are basis vectors of the square lattice. We set the lattice constant a to be equal to unity.

Local order parameter.—OP is to be calculated from the self-consistency equation

$$\Delta_{ij} = g_{ij} T \sum_{\varepsilon_n} \text{Tr}_4 [\hat{\tau}_- i \hat{\sigma}_y \check{G}_{ij}(\varepsilon_n)] , \quad (3)$$

where $\hat{\tau}_- = (\hat{\tau}_x - i \hat{\tau}_y)/2$. Eqs. (3) and (2) allow us to find the OP Δ_{ij} numerically.

We begin by considering a single perturbation of the pairing interaction of the form $f_i = \exp(-r/\lambda)/r$, where $r = \sqrt{i_x^2 + i_y^2 + z^2}$. However, the results do not depend qualitatively on the particular form of the perturbation and are only controlled by its effective width and height.

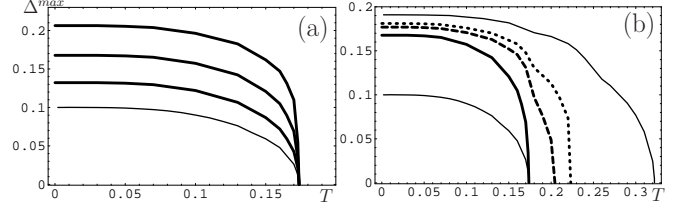


FIG. 1: (a) Dependence of the site-averaged OP maximal value Δ^{max} on temperature for $z = 0.5$ and $\lambda = 0.5$. $g^{max} = g_0 + \delta g^{max} = 0.857, 1.022$ and 1.187 from the bottom curve to the top one. (b) Evolution of $\Delta^{max}(T)$ dependence with increasing of the perturbation size for constant $g^{max} = 1.022$. $z = 0.5, \lambda = 0.5$ (solid line); $z = 2, \lambda = 2$ (dashed line) and $z = 3, \lambda = 3$ (dotted line). Bottom and top thin solid lines represent homogeneous bulk dependence $\Delta_0(T)$ for $g_b = 0.692$ and $g_b = 1.022$, respectively.

The dependence of the site-averaged OP maximal value $\Delta^{max} = (\Delta_{0,\hat{a}} + \Delta_{0,-\hat{a}} + |\Delta_{0,\hat{b}}| + |\Delta_{0,-\hat{b}}|)/4$ on temperature is presented in Fig.1. The left panel demonstrates the most spikier perturbation we consider: $z = 0.5$ and $\lambda = 0.5$. This perturbation has considerably non-zero value only at four bonds emanating from the central site. Here and below all the distances are measured in units of lattice constant. The different curves correspond to different heights of the perturbation: $g^{max} = g_b + \delta g^{max} = 0.857, 1.022$ and 1.187 from the bottom curve to the top one. The background pairing interaction is taken to be $g_b = 0.692$. The thin solid line represents the temperature behavior of the homogeneous order parameter without a perturbation added. We denote the critical temperature of the inhomogeneous sample by T_x in order to distinguish it from the background critical temperature T_b . If the perturbation size is very small (a few bonds), as in Fig. 1(a), the corresponding T_x practically does not differ from T_b . The physical reason for it is that small as compared to superconducting coherence length perturbations at the mean-field level cannot maintain superconductivity by themselves and only do this due to the superconductivity in the bulk. Then the bulk OP vanishes, the pairing correlations in the small area go to zero abruptly. On the other hand, the value of the zero-temperature OP Δ^{max} strongly enhances when the height of the perturbation grows. Therefore, local ratios Δ_{ij}/T_x can considerably exceed the homogeneous bulk value. For the parameters we consider in Fig. 1(a) $\Delta_0/T_b = 0.58$ and $\Delta^{max}/T_x = 0.76, 0.97$ and 1.19 from bottom to top.

When the size of the pairing interaction perturba-

tion increases, T_x grows and, correspondingly, the ratio Δ_{ij}/T_x starts to decline. Naturally, when the size of the enhanced pairing area becomes of the order of a few superconducting coherence lengths ξ_s , the bulk value of Δ_{ij}/T_x corresponding to $g = g_b + \delta g$ should be restored at the center of the cluster. The evolution of $\Delta^{max}(T)$ dependence with increasing of the perturbation size is illustrated in Fig. 1(b) for constant $g^{max} = 1.022$. For comparison the curve $\Delta_0(T)$ corresponding to this value of the pairing interaction is depicted in the same panel by the thin line. Therefore, large enough ratios Δ^{max}/T_x could be only obtained when the characteristic size of the OP enhanced area is considerably less than superconducting coherence length. However, the anomalous Green's function, which enters the self-consistency equation (3) always has the characteristic length of the order of $\xi_s \sim t/\Delta_0$ regardless of the particular parameter of the hamiltonian coursing the inhomogeneity. Consequently, the OP spacial profile follows the spacial profile of the coupling constant according to Eq. (3) except for very low tails extended to the distance of the order ξ_s due to the inhomogeneities of the anomalous Green's function. Therefore, we believe that the large enough ratio Δ_{ij}/T_x can only be obtained (at least in the framework of mean-field BCS theory with temperature-independent coupling constant) by assuming the atomic-scale inhomogeneity of the pairing interaction strength.

Now we turn to discussion of more realistic situation, when many pair interaction scatterers are present in the sample. It is worth noting that in our mean-field treatment we neglect OP phase, which is a strongly fluctuating quantity in short coherence length high- T_c superconductors and, especially, in the inhomogeneous situation. In the present paper we only study local pairing and do not concern the global transition temperature T_c , which is controlled by the phase fluctuations.

We have considered a 21×21 sites square as a perturbation described by the T-matrix. The coupling constant outside this square is set to be $g_b = 0.692$. Fig. 2 shows the particular example. The pairing interaction scatterers corresponding to $\lambda = 1.5$ and $z = 1$ are distributed in the square with the concentration $n = 0.078$. The background coupling constant in the square and the height of the individual perturbation are chosen to give the same average as outside the square: $g_0 = 0.45$, δg is randomly distributed in the range $0.70 - 1.35$.

The resulting distribution of zero-temperature OP is presented in Fig. 2(a). As it was described earlier for the single perturbation, the spacial profile of the OP inhomogeneity mainly follows that one of the coupling constant. The dependence of the site-averaged $\Delta_i(T)$ for the marked sites is plotted in Fig. 2(b).

Local density of states.—STM technique measures the local differential conductance, and the thermally smeared LDOS, described by the expression

$$dI/dV = \int_{-\infty}^{\infty} d\varepsilon (df(\varepsilon + V)/dV) \rho_i(\varepsilon, T), \quad (4)$$

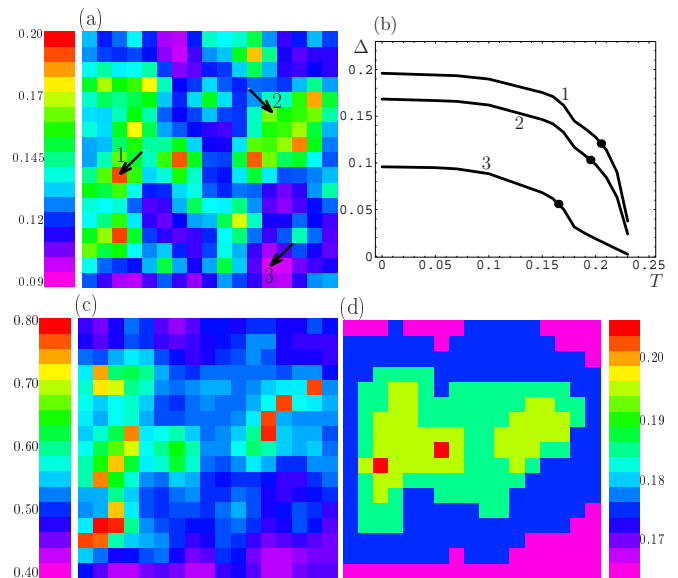


FIG. 2: (Color online) (a) Zero-temperature distribution of the site-averaged OP. (b) The temperature dependence of the site-averaged OP for the sites marked by the arrows in (a). The bold circles show T_p corresponding to these locations. (c) Low-temperature gap map. (d) T_p -map.

can be extracted from these measurements. Here $\rho_i(\varepsilon, T) = -(1/\pi)\text{Im}G_{ii}^R(\varepsilon, T)$ is the local density of states, $f(\varepsilon)$ is Fermi distribution function and V is voltage applied between the STM tip and the sample. For the homogeneous situation in the framework of mean-field weak-coupling BCS theory the distance between the coherence peaks $2\Delta_g$ in the conductance spectra directly connected to the OP by the simple relation $\Delta_g \approx 3.7\Delta(T=0)$ for the particular lattice parameters we have chosen.

For an inhomogeneous system, where the characteristic size of the patch $\lesssim \xi$, there is no any direct simple relationship between the local OP and the local gap Δ_g . One can only conclude from the numerical calculations^{7,17} that for regions, where the OP is enhanced from the background, the gap gets wider and the peak height is suppressed compared to the average value. It is worth noting that, unlike the homogeneous situation, this peak does not represent the maximal superconducting gap on the Fermi surface, but rather originates from the spectral weight transfer from the nearby van Hove singularity due to the Andreev scattering processes. Otherwise, if the OP in a cluster is less than that one in the background, the narrow and high Andreev resonant peaks develop in the cluster region resulting in diminishing of the gap region. For this reason we investigate not only the OP distribution, but also the experimentally measurable thermally smeared LDOS, which has a maximum at $V = \Delta_g$. The corresponding low-temperature gap map is represented in Fig. 2(c) for the model sample considered above.

Experimentally¹ the temperature $T_p(i)$ of the gap disappearing for the particular location in the sample has

been determined using the criterion $dI/dV(V = 0) \geq dI/dV$ (for all $V \geq 0$). Using the above criterion we calculated the distribution $T_p(i)$ from the thermally smeared LDOS curves. The corresponding T_p -map is represented in Fig. 2(d). In addition, for the locations, marked in Fig. 2(a), appropriate T_p is shown by bold circles in Fig. 2(b). Although in our model the OP vanishes at the temperature T_x , which is the same for the entire sample, it is seen that the temperature T_p is strongly position-dependent and considerably lower than T_x for the most part of the sample. There are two main physical reasons for this effect: (i) LDOS is essentially nonlocal (on the atomic scale) quantity with the characteristic size of order of ξ_s . This fact leads to the partial averaging of essentially different gaps over the region $\sim \xi_s^2$ and spacial redistribution of the spectral weight due to Andreev scattering processes. (ii) thermal broadening of the LDOS further washes out the conductance peaks. It is worth noting that the LDOS $\rho(\varepsilon, T)$ taking without thermal smearing results in higher values of the local gap vanishing temperature. This is demonstrated in the right panel of Fig. 3.

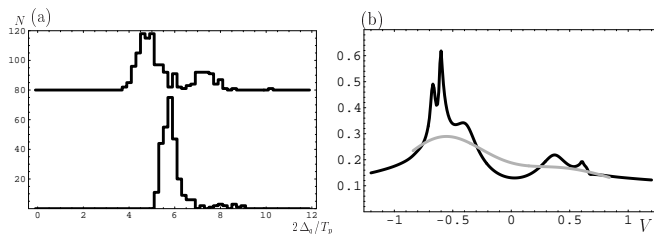


FIG. 3: (a) The probability distribution to find the particular value for $2\Delta_g(i)/T_p(i)$. The bottom curve represents the same model sample as in Fig. 2. The top one corresponds to another example with $n = 0.052$, $\lambda = 2$, $z = 0.5$, $g_0 = 0.35$ and $\delta g = 0.8$. The offset is for clarity. (b) LDOS (black curve) in comparison with the thermally smeared LDOS (gray curve) for a particular location and $T = 0.18$.

The probability distribution to find the particular value for $2\Delta_g(i)/T_p(i)$ in the model sample considered above is plotted in the left panel of Fig. 3 (bottom curve). It is seen that the distribution is quite narrow, that is this ratio is practically independent on the particular location in the sample. In the framework of our model this result can be only obtained if the scatterers are distributed in the sample randomly, but the additional restriction is imposed: they influence each other in the sense that the distance between them cannot be too small. If this re-

striction is not imposed and the scatterers are distributed quite randomly, the ratio $2\Delta_g(i)/T_p(i)$ is obtained to be more position-dependent. This is demonstrated for another model sample in the left panel of Fig. 3 (top curve). This sample differs from the considered above by the shape of an individual scatterer and by their concentration. However, we have investigated a number of model samples and checked that the $2\Delta_g(i)/T_p(i)$ distribution shape is only determined by the extent of uniformity of the scatterers.

The averaged ratio $2\Delta_g/T_p$ we calculated is equal to 5.9. It is larger than that one for a homogeneous situation corresponding to the same normal state hamiltonian $2\Delta_g/T_p = 4.7$ but is smaller than experimentally measured one¹. However, it is obvious from the above analysis that the underlying ratio of the OP to the critical temperature Δ_{ij}/T_x gets larger as the height of the perturbation increases and its width diminishes. The manifestation of the effect in LDOS, and, consequently, the behavior of the experimentally measured ratio $2\Delta_g/T_p$ is not so straightforward²⁵ and strongly depends on the particular choice of the lattice parameters. The point is that for the inhomogeneous situation the peak in the LDOS results from the Andreev scattering processes between the background superconducting coherence peak and nearby van Hove singularity, as it was already mentioned above. So, the position Δ_g of the LDOS peak strongly depends on the energy distance between them in comparison to the strength of the individual scatterer.

In conclusion, we have studied the influence of the atomic-scale inhomogeneities of the pairing interaction strength on the OP distribution and the LDOS in the framework of mean-field BCS theory. It is found that the ratio of the local low-temperature gap in differential conductance spectra to the local temperature of vanishing the gap $2\Delta_g/T_p$ can take large enough values compared to the homogeneous one. This ratio is position-independent in case if the off-diagonal scatterers are distributed rather uniformly and practically independent on their concentration in wide range of the concentrations. On the other hand, it is quite sensitive to characteristic size and height of the individual pairing interaction scatterer and to the choice of the lattice parameters.

Acknowledgments. The support by RFBR Grant 05-02-17731 (A.M.B.) and the programs of Physical Science Division of RAS is acknowledged. I.V.B. was also supported by the Russian Science Support Foundation and RF Presidential Grant No.MK-4605.2007.2

* Electronic address: bobkova@issp.ac.ru

¹ K. Gomes *et al.*, Nature(London), **447**, 569 (2007).

² T. Cren *et al.*, Phys. Rev. Lett. **84**, 147 (2000).

³ S.H. Pan *et al.*, Nature (London) **413**, 282 (2001).

⁴ C. Howard *et al.*, Phys. Rev. B **64**, 100504 (2001).

⁵ K.M. Lang *et al.*, Nature (London) **415**, 412 (2002).

⁶ K. McElroy *et al.*, Science **309**, 1048 (2005).

⁷ A.C. Fang *et al.*, Phys. Rev. Lett. **96**, 017007 (2006).

⁸ I. Martin and A.V. Balatsky, Physica C **357**, 46 (2001).

⁹ Z. Wang *et al.*, Phys.Rev. B, **65**, 064509 (2002).

- ¹⁰ Q.H. Wang *et al.*, Phys.Rev. B, **65**, 054501 (2002).
¹¹ S.A. Kivelson *et al.*, Rev.Mod.Phys. **75**, 1201 (2003).
¹² W.A. Atkinson, Phys. Rev. B, **71**, 024516, (2005).
¹³ G. Alvarez *et al.*, Phys. Rev. B **71**, 014514 (2005).
¹⁴ A. Ghosal *et al.*, Phys. Rev. B **72**, 220502(R) (2005).
¹⁵ D. Podolsky *et al.*, Phys. Rev. B **67**, 094514 (2003).
¹⁶ H.D. Chen *et al.*, Phys. Rev. Lett. **93**, 187002 (2004).
¹⁷ T. Nunner *et al.*, Phys. Rev. Lett. **95**, 177003 (2005).
¹⁸ Brian M. Andersen *et al.*, Phys. Rev. B **74**, 060501(R) (2006).
¹⁹ T. Timusk and B. Statt, Rep. Prog. Phys. **62**, 61 (1999).
²⁰ M.R. Norman *et al.*, Adv. Phys. **54**, 715 (2005).
²¹ P.A. Lee *et al.*, Rev. Mod. Phys. **78**, 17 (2006).
²² A.J. Millis, Science **314**, 1888 (2006).
²³ A. Cho, Science **314**, 1072 (2006).
²⁴ M. Franz *et al.*, Phys. Rev. B, **56**, 7882 (1997).
²⁵ I.V. Bobkova and A.M. Bobkov, in preparation.